

## Proton Transfer

International Edition: DOI: 10.1002/anie.201806787  
German Edition: DOI: 10.1002/ange.201806787

## Ultrafast Dynamics of a “Super” Photobase

Wei Sheng<sup>†</sup>, Muath Nairat<sup>†</sup>, Patrick D. Pawlaczyk, Elizabeth Mroczka, Benjamin Farris, Ehud Pines, James H. Geiger, Babak Borhan,<sup>\*</sup> and Marcos Dantus<sup>\*</sup>

**Abstract:** Molecular reactivity can change dramatically with the absorption of a photon due to the difference of the electronic configurations between the excited and ground states. Here we report on the discovery of a modular system (Schiff base formed from an aldehyde and an amine) that upon photoexcitation yields a more basic imine capable of intermolecular proton transfer from protic solvents. Ultrafast dynamics of the excited state conjugated Schiff base reveals the pathway for proton transfer, culminating in a 14-unit increase in  $pK_a$  to give the excited state  $pK_a^* > 20$  in ethanol.

Proton transfer remains one of the most important and fundamental steps in chemical and biological processes.<sup>[1]</sup> Some weak acids and bases exhibit an increase in their acidity ( $pK_a^* < pK_a$ ) or basicity ( $pK_a^* > pK_a$ ) upon photoexcitation; such compounds are known as photoacids or photobases, respectively (Figure 1). Since the early work on excited state proton transfer (ESPT) processes by Förster and Weller,<sup>[2]</sup> a large number of experimental and theoretical studies have investigated the underlying dynamics and principles.<sup>[3]</sup> This stems from both the fundamental interest in understanding ESPT dynamics and the exploitation of photoacids as a functional tool in areas such as triggering protein folding<sup>[4]</sup> and pH jumps,<sup>[5]</sup> as well as probing micro-solvation<sup>[6]</sup> and regulating enzymatic reactions using light,<sup>[7]</sup> to name a few. Recently, photoacids, an example of which is shown in Figure 1,<sup>[8]</sup> have found more extensive applications in chemical sensors, proton-transfer lasers, organic light-emitting diodes,<sup>[9]</sup> dye-sensitized ion exchange membranes,<sup>[10]</sup> and large Stokes shift fluorescent proteins.<sup>[11]</sup> A recent example highlights photoacids in the enantioselective protonation of silyl enol ethers leading to enantioenriched  $\alpha$ -substituted carbonyls.<sup>[12]</sup> In contrast, the literature on photobases is scarce and limited to heterocyclic amines such as acridines,<sup>[13]</sup> 3-styrylpyridines,<sup>[14]</sup> aminoanthraquinones,<sup>[15]</sup>

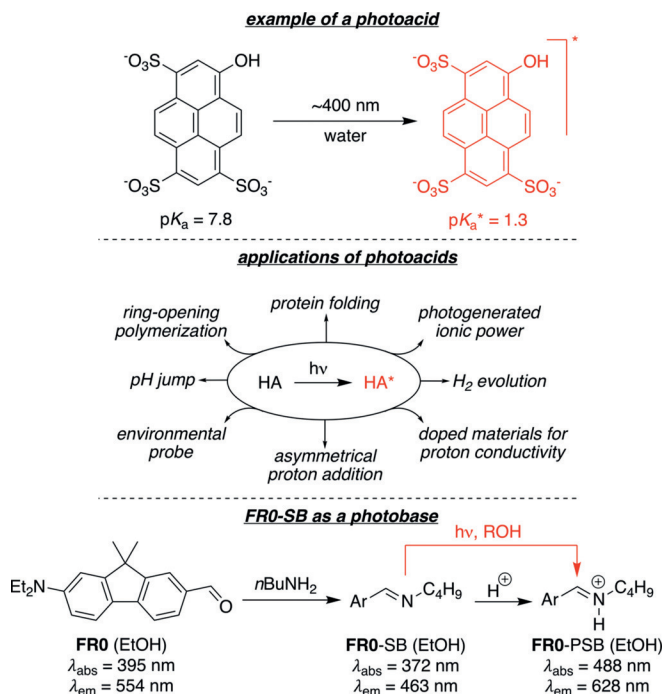


**Figure 1.** Photoacids are prevalent in a variety of applications, as they offer control of function via a light prompt. FR0-SB is one of few photobases known, formed in a modular manner from the reaction of FR0 aldehyde with an amine.

Schiff bases,<sup>[16]</sup> and quinolines.<sup>[17]</sup> Curcumin,<sup>[18]</sup> xanthone,<sup>[19]</sup> and other bifunctional photoacids have been sporadically reported to show certain photobasic features.<sup>[19,20]</sup> These photobases are different from photobase generators, which are generated upon light irradiation of their salts and have the drawback of being irreversible with slow proton transfer rates.<sup>[21]</sup>

The prevalence of photoacids has led to their exploitation in a number of avenues, however the paucity of photobases has hampered investigations into their utility. Nonetheless, the ability to control the basicity of an agent via photoexcitation can be as important as those demonstrated with photoacids. The term super-photoacidity was coined by Tolbert and co-workers for photoacids that are strong enough to photo-dissociate in non-aqueous solutions.<sup>[22]</sup> The term stemmed from work by Carmeli et al,<sup>[23]</sup> and Huppert, Tolbert and co-workers.<sup>[24]</sup> Similarly, one may formally introduce the term “super-photobasicity” for photobases, which are strong enough to abstract protons from non-aqueous solvents such as alcohols. This definition is general and does not depend on an arbitrary  $pK_a$  value or change in  $pK_a$  value upon photoexcitation. Here, we report on the photobasic properties and proton transfer dynamics of FR0-

<sup>[\*]</sup> W. Sheng,<sup>[†]</sup> M. Nairat,<sup>[†]</sup> P. D. Pawlaczyk, E. Mroczka, B. Farris, Prof. Dr. J. H. Geiger, Prof. Dr. B. Borhan, Prof. Dr. M. Dantus Department of Chemistry, Michigan State University E. Lansing, MI 48824 (USA)  
E-mail: babak@chemistry.msu.edu  
dantus@msu.edu

Prof. Dr. E. Pines  
Department of Chemistry, Ben-Gurion University of the Negev  
POB 653, Beer Sheva 84105 (Israel)

Prof. Dr. M. Dantus  
Department of Physics and Astronomy, Michigan State University  
East Lansing, MI 48824 (USA)

<sup>[†]</sup> These authors contributed equally to this work.

Supporting information and the ORCID identification number(s) for the author(s) of this article can be found under:  
<https://doi.org/10.1002/anie.201806787>.

SB, a conjugated Schiff base (SB) obtained via the imine formation between the strong solvatochromic dye **FR0** (a fluorene based aldehyde) with *n*-butylamine (Figure 1, see Scheme S1 in the Supporting Information for the synthesis), a modular system that can be synthesized using a variety of aldehydes and amines.<sup>[25]</sup> Upon photoexcitation of **FR0-SB** in ethanol, fluorescence of the protonated Schiff base (PSB) is observed, which warrants the consideration of **FR0-SB** as a super photobase.

**FR0-SB** in acetonitrile (ACN) has an absorption centered at 369 nm and an emission maximum at 479 nm (Figure 2a). When **FR0-SB** is dissolved in protic solvents, dual emission bands are observed with maxima at 463 nm and 628 nm for EtOH (Figure 2b, see Figure S1 for spectra in MeOH and *n*-BuOH). The emergence of the red emission in protic solvents is ascribed to the protonated Schiff base (PSB) of **FR0** that forms upon excitation. To confirm, the **FR0-SB** was acidified by addition of dilute HClO<sub>4</sub> to protonate the imine in EtOH, leading to a large red shift in the absorption spectrum (from 372 nm to 488 nm, Figure 2b). Accordingly, the fluorescence becomes limited to the low energy emission with a 630 nm maximum, which confirms the assignment of the protonated form of **FR0-SB** (**FR0-PSB**).

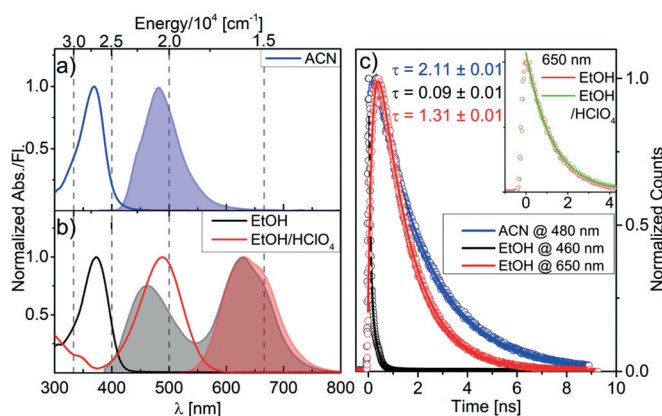


**Figure 2.** Absorption (solid line) and emission (shaded area) spectra of **FR0-SB** in a) ACN (blue), b) EtOH (black) and acidified EtOH (red). c) TCSPC traces with single exponential fits for **FR0-SB** near the emission maxima when dissolved in ACN (blue) and EtOH (black and red). Inset shows that the red emission trace at 650 nm of **FR0-SB** is identical to the **FR0-PSB** emission with 400 nm excitation.

Due to the rapid decay of the excited state that leads to the rapid protonation of **FR0-SB**, time-resolved fluorescence measurements were carried out by picosecond time-correlated single photon counting (TCSPC) to further confirm the nature of the red emission (Figure 2c). The emission in ACN exhibits a single exponential decay with a 2.11 ns lifetime, whereas in EtOH, the blue emission lifetime decreases sharply to ca. 89 ps. The decrease in the blue-emission lifetime can be explained by the competing intermolecular proton transfer from the solvent to **FR0-SB** in the excited state, a process that is not possible in ACN. The excited **FR0-SB** acts as a photobase that readily abstracts a proton from EtOH to form the iminium, which has an emission maximum

at 628 nm. The red emission of **FR0-SB** in EtOH displays an identical decay trace to that of the iminium formed in EtOH/HClO<sub>4</sub> solution with a lifetime of 1.31 ns (Figure 2c inset, for detailed TCSPC traces see Figure S2).

The change in  $pK_a$  upon excitation is determined using the Förster equation,<sup>[2a,3c]</sup> where  $pK_a^*$  and  $pK_a$  are the excited state and ground state logarithmic acidity constants, respectively;  $h\nu$  is the energy of the 0-0 electronic transition of the base and its conjugate acid (see Eq. 1). The 0-0 transition energies were estimated as 24450 cm<sup>-1</sup> and 17890 cm<sup>-1</sup> from the corresponding crossing points of the absorption and emission spectra for both **FR0-SB** and **FR0-PSB**, respectively (Figure 2b).<sup>[26]</sup> The calculated increase in  $pK_a$  is 13.8 units. While  $pK_a$  changes up to 14 units have been reported for photoacids,<sup>[20]</sup> to the best of our knowledge the largest  $pK_a$  change reported for a photobase is 10.8 for 5-aminoquinoline.<sup>[27]</sup> With the  $\Delta pK_a$  in hand, calculation of the excited state  $pK_a^*$  requires an estimate for the ground state  $pK_a$  of **FR0-PSB**. Although a good estimate for the  $pK_a$  in EtOH can be derived from the  $pK_a$  of the imine in water, this was hampered by the insoluble nature of **FR0-SB** in water. Note that the  $pK_a$  of ammonium salt is generally elevated by ~3 units when dissolved in ethanol instead of water.<sup>[28]</sup> Therefore, we resorted to an indirect measurement of the  $pK_a$  via quantifying the mole fraction of each species by multi-variant linear regression with known extinction coefficients as a function of wavelengths (UV/Vis analysis), generated between the acid-base reaction of **FR0-SB** with  $\alpha$ -naphthylammonium in EtOH as described in a previously reported procedure.<sup>[29]</sup> **FR0-PSB** shows a 0.23 unit lower  $pK_a$  than that of  $\alpha$ -naphthylammonium in EtOH. The  $pK_a$  of  $\alpha$ -naphthylammonium in water is 3.9, thus, its  $pK_a$  in EtOH is estimated at 6.9. Considering the difference in  $pK_a$  values for  $\alpha$ -naphthylammonium and **FR0-PSB**, the  $pK_a$  of the latter in EtOH is estimated to be 6.7. This results in an estimated excited state  $pK_a^*$  of 21 for **FR0-SB**. The large change in  $pK_a$ , occurring upon excitation, is ascribed to the increased electron density, and thus an amplified negative polarity on the imine nitrogen atom in the excited state (see Figure S3).

$$pK_a^* - pK_a = (h\nu_1 - h\nu_2)/2.3RT \quad (1)$$

The relative ratio of the areas under the emission bands for the protonated **FR0-PSB** divided by **FR0-SB** in ethanol is 1.45. We have also estimated the relative ratio of quantum yields between **FR0-SB** and **FR0-PSB** as 3.3 (see Figure S4 and S5). Therefore, one can deduce a relative population ratio of 4.8 between **FR0-PSB** and **FR0-SB** in ethanol. Since **FR0-SB** emission at 460 nm is associated with a lifetime of 89 ps, we surmise that the protonation step is associated with a lifetime of ~18 ps. However, the observed rise in the fluorescence at 650 nm was 197 ps; the large difference can be attributed to an intermediate state between the initial excited state abstracting the proton and the final protonated species that may have a nanosecond radiative lifetime but has a low quantum yield due to the fast conversion (200 ps) to the final state.

The early dynamics can be further investigated using transient absorption as shown in Figure 3. Upon excitation at

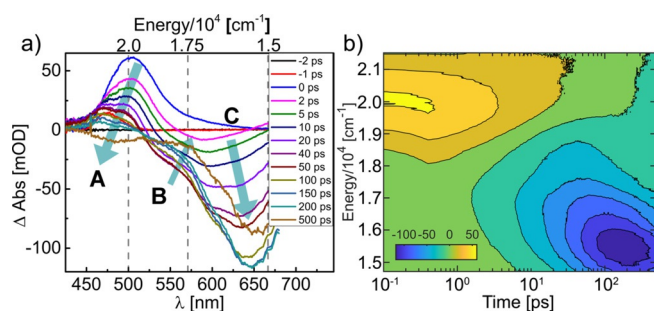


**Figure 3.** a) Transient absorption spectra of **FR0-SB** at various time intervals after excitation in EtOH. Labeled arrows show the steps during the ESPT process. b) Energy progression during the proton transfer process.

400 nm, a decrease in absorption (positive signal) around 500 nm ( $20000\text{ cm}^{-1}$ ) was observed initially, which is attributed to excited state absorption (ESA) of **FR0-SB**. The ESA signal decays quickly (arrow **A** in Figure 3a) and is accompanied by a transient negative signal centered at 588 nm ( $17000\text{ cm}^{-1}$ , arrow **B**) that gives rise to another negative signal initially centered at 630 nm ( $15870\text{ cm}^{-1}$ , arrow **C**) and shifts to lower energy over time. The negative signal at 630 nm persists longer than 500 ps and is assigned as the stimulated emission (SE) from **FR0-PSB**. The transient signal at 588 nm is ascribed to the SE from an intermediate species that forms during the course of the intermolecular proton transfer. The intermediate is thought to be a caged complex between **FR0-SB** and the solvent molecule with a partial transfer of the proton (vide infra) prior to the full proton transfer process that is observed in the intermolecular proton transfer of photoacids.<sup>[3a,20]</sup>

Transient absorption in the absence of a proton transfer event, such as in ACN, shows that ESA and SE appear soon after excitation (Figure S6) since both correspond to the non-protonated form. Both ESA and SE signals are long-lived and can be fit to a biexponential decay with a long component of about 2.1 ns corresponding to the lifetime of the excited state and a short 26 to 30 ps component that is ascribed to conformational changes of the molecule upon excitation. The 26 ps decay component is also observed when exciting **FR0-PSB** (in EtOH/ $\text{HClO}_4$ ), confirming its nature as an intramolecular mode from **FR0-SB** regardless of its protonation status (Figure S7).

A more complete description of the experimental transient absorption data in EtOH is best obtained using a four-level sequential global analysis model.<sup>[30]</sup> The evolution associated spectra obtained are provided in Figure S8. As stated previously, excitation in ACN (**I** → **III**, Figure 4) leads to a long-lived excited state (2.11 ns), while proton transfer in EtOH drastically reduces the excited state lifetime of **III** in the protic solvent (89 ps in EtOH). The model shows that the first component, which is the ESA of **FR0-SB** centered around 500 nm ( $20000\text{ cm}^{-1}$ ), decays with a 15.8 ps time constant (see **III** → **IV**, Figure 4), which agrees with the previously deduced  $\approx 18$  ps from steady state spectra and the TCSPC measured lifetime. This timescale is in agreement with the average dielectric relaxation of EtOH (16 ps).<sup>[31]</sup> This

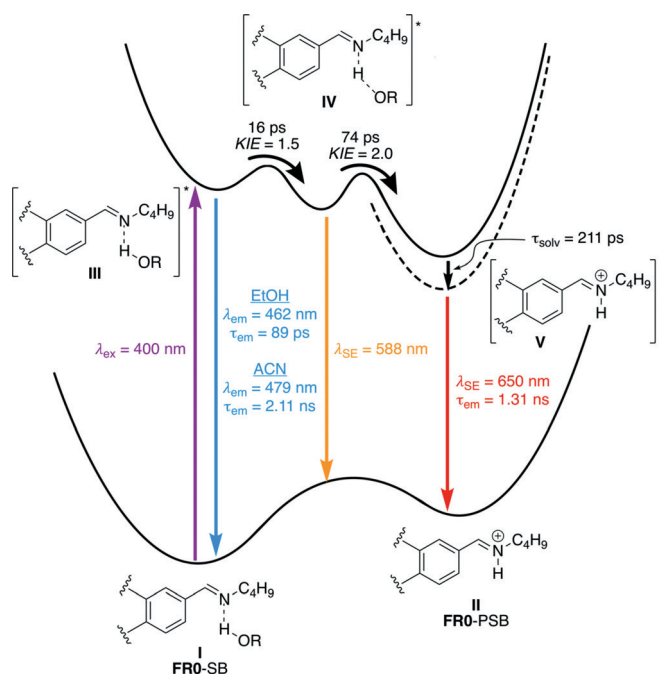


**Figure 4.** The observed intermolecular ESPT dynamics in EtOH along with the associated time constants for the steps as obtained from global analysis (black) and the TCSPC data (colored).

decay is accompanied with a rise in the second component featuring a broad SE signal centered at 588 nm ( $17000\text{ cm}^{-1}$ ), presumably the partially protonated state depicted as **IV**, decaying with a 73.9 ps time constant to yield the excited PSB form of **FR0** (**V**). It is worth noting that the partially protonated state **IV** is not emissive and is only observed by stimulated emission. Based on these time constants, we infer that the dielectric relaxation of the solvent is coupled with the formation of an intermediate species prior to the full proton transfer step. Characterized by the **FR0-PSB** SE feature with maxima around 630–660 nm ( $15870$ – $15150\text{ cm}^{-1}$ ), the final step is best described with two components. Considering the similarities between the last two components (see Figure S7, for spectra of components three and four) we stipulate them as solvation of the protonated form **V**. This step occurs on a 211 ps time scale, which agrees with the observed rise time in the TCSPC data at 650 nm (197 ps, see Figure S2b). The last component is long lived and decays with a 1.15 ns time constant, a value in agreement with the protonated **FR0-SB** lifetime (1.31 ns) that was previously determined using TCSPC (Figure 2c).

Similar photophysical behavior is observed when **FR0-SB** is dissolved in MeOH (Figure S9). The global analysis model shows that the ESA signal from the non-protonated form decays to form the partially-transferred proton complex on a 2.9 ps timescale, also in agreement with the average dielectric solvation time of MeOH (5 ps).<sup>[31]</sup> The protonated **FR0-SB** is formed on a 27.1 ps timescale according to the global analysis model.

As depicted in Figure 5, the global analysis deduced pathway was further confirmed using the transient absorption traces at selected wavelengths of **FR0-SB** in EtOH and EtOD



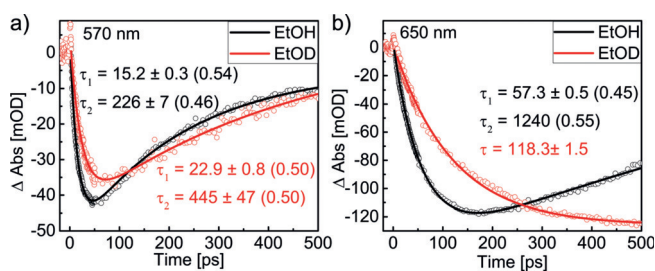


**Figure 5.** Transient absorption traces at a) 570 nm where SE from the intermediate formation is observed, and b) 650 nm where SE from the protonated **FR0-SB** can be seen while dissolved in EtOH (black) and EtOD (red). Biexponential decay constants are given in the inset along with the pre-exponential factors in parentheses. An isotope effect of 1.5 is observed during the formation of the partially-transferred proton intermediate while an isotope effect of 2 is observed during the final protonated form formation. Note, as the result of its apparent long-lived nature, lifetime of the 650 nm decay for the EtOD experiment could not be determined.

([D<sub>6</sub>]ethanol). The formation of the intermediate, observed through the SE signal at 570 nm (Figure 5a), is coupled to dielectric solvent relaxation and occurs with a 15.2 ps time constant, in close agreement with the intermediate formation time as determined by the global analysis model (15.8 ps).

The second trace at 650 nm, which is the SE from the protonated **FR0-SB**, appears with a 57.3 ps time constant and is ascribed to the dissociation of the intermediate to form **FR0-PSB** (Figure 5b). It is more accurately measured by the global analysis, which gives a 73.9 ps time constant. Analysis of the transient absorption for the decay of each species in EtOH and EtOD ([D<sub>6</sub>]ethanol) provides kinetic isotope effect (KIE) for each individual step. The initial 1.5 KIE is supportive of a hydrogen-bonded complex with partial transfer of the proton to the imine. The faster decay of the first transient intermediate in comparison to the second step suggests that the second measured KIE is independent of the first, as one would not expect a population of the transient species to accumulate. The second, greater KIE (2.0) is suggestive of the actual bond breaking event that leads to the fully protonated species (see Figure 4). A greater isotope effect is observed in MeOD ([D<sub>4</sub>]MeOH) as shown in Figures S10 and S11.

In summary, a modular molecular system (imine formation via the reaction of an aldehyde with an amine), with the flexibility to easily probe structural and electronic factors in future studies, shows a remarkable ability to increase its basicity upon photoexcitation. The ability to electively stimulate proton abstraction with light during reactions will find itself useful in an array of disciplines. Possible applications include, super photobase proton abstraction from acids weaker than water, protein conformational changes, selective functionalization of unactivated C–H bonds, and potentially assisting in water splitting. Furthermore, the large apparent Stokes shift and strong fluorescence will be useful for imaging and displays. The variety and expansive nature of potential applications for super photobases indicates their importance for further studies.

## Acknowledgements

Support was provided by the National Science Foundation (CHE-1464807) to M.D. and the National Institute of Health (GM101353) to J.H.G. and B.B. We would like to thank Prof. Gary Blanchard (MSU) for allowing us to bring our femto-second laser to his TCSPC setup so that we could acquire the fluorescence lifetimes reported with an instrument response time shorter than 50 ps. We thank Dr. Joris Snellenburg for help in using Glotaran.

## Conflict of interest

The authors declare no conflict of interest.

**Keywords:** excited state · fluorene · photobase · proton transfer · transient spectroscopy

**How to cite:** *Angew. Chem. Int. Ed.* **2018**, *57*, 14742–14746

*Angew. Chem.* **2018**, *130*, 14958–14962

- [1] J. T. Hynes, P. J. P. Klinman, H.-H. Limbach, R. L. Schowen, *Hydrogen-Transfer Reactions*, Wiley-VCH, Weinheim, **2007**.
- [2] a) A. Weller, *Z. Elektrochem.* **1952**, *56*, 662–668; b) T. Förster, *Z. Elektrochem.* **1950**, *54*, 531–535.
- [3] a) T. Kumpulainen, B. Lang, A. Rosspeintner, E. Vauthey, *Chem. Rev.* **2017**, *117*, 10826–10939; b) N. Agmon, *J. Phys. Chem. A* **2005**, *109*, 13–35; c) L. M. Tolbert, K. M. Solntsev, *Acc. Chem. Res.* **2002**, *35*, 19–27; d) E. Pines, D. Pines in *Ultrafast Hydrogen Bonding Dynamics and Proton Transfer Processes in the Condensed Phase* (Eds.: T. Elsaesser, H. J. Bakker), Springer Netherlands, Dordrecht, **2002**, pp. 155–184; e) A. Douhal, F. Lahmani, A. H. Zewail, *Chem. Phys.* **1996**, *207*, 477–498; f) L. G. Arnaut, S. J. Formosinho, *J. Photochem. Photobiol. A* **1993**, *75*, 1–20; g) J. F. Ireland, P. A. H. Wyatt, *Adv. Phys. Org. Chem.* **1976**, *12*, 131–221; h) A. Rosspeintner, B. Lang, E. Vauthey, *Annu. Rev. Phys. Chem.* **2013**, *64*, 247–271; i) O. F. Mohammed, D. Pines, J. Dreyer, E. Pines, E. T. J. Nibbering, *Science* **2005**, *310*, 83–86.
- [4] S. Abbruzzetti, E. Crema, L. Masino, A. Vecli, C. Viappiani, J. R. Small, L. J. Libertini, E. W. Small, *Biophys. J.* **2000**, *78*, 405–415.
- [5] a) P. Wan, D. Shukla, *Chem. Rev.* **1993**, *93*, 571–584; b) E. Pines, D. Huppert, *J. Phys. Chem.* **1983**, *87*, 4471–4478; c) M. Gutman, D. Huppert, E. Pines, *J. Am. Chem. Soc.* **1981**, *103*, 3709–3713.
- [6] J.-Y. Shen, W.-C. Chao, C. Liu, H.-A. Pan, H.-C. Yang, C.-L. Chen, Y.-K. Lan, L.-J. Lin, J.-S. Wang, J.-F. Lu, S. C.-W. Chou, K.-C. Tang, P.-T. Chou, *Nat. Commun.* **2013**, *4*, 2611.
- [7] H. Peretz-Soroka, A. Pevzner, G. Davidi, V. Naddaka, M. Kwiat, D. Huppert, F. Patolsky, *Nano Lett.* **2015**, *15*, 4758–4768.
- [8] a) E. Pines, D. Huppert, *J. Am. Chem. Soc.* **1989**, *111*, 4096–4097; b) D. Pines, E. Pines, *J. Chem. Phys.* **2001**, *115*, 951–953.
- [9] J. E. Kwon, S. Y. Park, *Adv. Mater.* **2011**, *23*, 3615–3642.
- [10] W. White, C. D. Sanborn, D. M. Fabian, S. Ardo, *Joule* **2018**, *2*, 94–109.
- [11] a) K. D. Piatkevich, V. N. Malashkevich, S. C. Almo, V. V. Verkhusha, *J. Am. Chem. Soc.* **2010**, *132*, 10762–10770; b) K. D. Piatkevich, J. Hulit, O. M. Subach, B. Wu, A. Abdulla, J. E. Segall, V. V. Verkhusha, *Proc. Natl. Acad. Sci. USA* **2010**, *107*, 5369–5374; c) K. D. Piatkevich, V. N. Malashkevich, K. S. Morozova, N. A. Nemkovich, S. C. Almo, V. V. Verkhusha, *Sci. Rep.* **2013**, *3*, 1847.
- [12] A. Das, S. Ayad, K. Hanson, *Org. Lett.* **2016**, *18*, 5416–5419.

- [13] a) E. T. Ryan, T. Xiang, K. P. Johnston, M. A. Fox, *J. Phys. Chem. A* **1997**, *101*, 1827–1835; b) E. Pines, D. Huppert, M. Gutman, N. Nachliel, M. Fishman, *J. Phys. Chem.* **1986**, *90*, 6366–6370.
- [14] G. Favaro, U. Mazzucato, F. Masetti, *J. Phys. Chem.* **1973**, *77*, 601–604.
- [15] T. Yatsuhashi, H. Inoue, *J. Phys. Chem. A* **1997**, *101*, 8166–8173.
- [16] A. Jiménez-Sánchez, R. Santillan, *Analyst* **2016**, *141*, 4108–4120.
- [17] N. Munitz, Y. Avital, D. Pines, E. T. J. Nibbering, E. Pines, *Isr. J. Chem.* **2009**, *49*, 261–272.
- [18] K. Akulov, R. Simkovitch, Y. Erez, R. Gepshtein, T. Schwartz, D. Huppert, *J. Phys. Chem. A* **2014**, *118*, 2470–2479.
- [19] B. S. Vogt, S. G. Schulman, *Chem. Phys. Lett.* **1983**, *97*, 450–453.
- [20] R. Simkovitch, K. Akulov, S. Shomer, M. E. Roth, D. Shabat, T. Schwartz, D. Huppert, *J. Phys. Chem. A* **2014**, *118*, 4425–4443.
- [21] K. Suyama, M. Shirai, *Prog. Polym. Sci.* **2009**, *34*, 194–209.
- [22] K. M. Solntsev, D. Huppert, N. Agmon, L. M. Tolbert, *J. Phys. Chem. A* **2000**, *104*, 4658–4669.
- [23] I. Carmeli, D. Huppert, L. M. Tolbert, J. E. Haubrich, *Chem. Phys. Lett.* **1996**, *260*, 109–114.
- [24] D. Huppert, L. M. Tolbert, S. Linares-Samaniego, *J. Phys. Chem. A* **1997**, *101*, 4602–4605.
- [25] O. A. Kucherak, P. Didier, Y. Mély, A. S. Klymchenko, *J. Phys. Chem. Lett.* **2010**, *1*, 616–620.
- [26] B. Marciniak, H. Kozubek, S. Paszyc, *J. Chem. Educ.* **1992**, *69*, 247–249.
- [27] E. W. Driscoll, J. R. Hunt, J. M. Dawlaty, *J. Phys. Chem. Lett.* **2016**, *7*, 2093–2099.
- [28] a) Y. Maitani, M. Nakagaki, T. Nagai, *Int. J. Pharm.* **1991**, *74*, 105–114; b) L. D. Goodhue, R. M. Hixon, *J. Am. Chem. Soc.* **1934**, *56*, 1329–1333.
- [29] A. Kütt, I. Leito, I. Kaljurand, L. Sooväli, V. M. Vlasov, L. M. Yagupolskii, I. A. Koppel, *J. Org. Chem.* **2006**, *71*, 2829–2838.
- [30] J. J. Snellenburg, S. Laptinok, R. Seger, K. M. Mullen, I. H. M. van Stokkum, *J. Stat. Soft.* **2012**, *49*, 1–22.
- [31] M. L. Horng, J. A. Gardecki, A. Papazyan, M. Maroncelli, *J. Phys. Chem.* **1995**, *99*, 17311–17337.

Manuscript received: June 12, 2018

Revised manuscript received: July 26, 2018

Accepted manuscript online: August 27, 2018

Version of record online: October 12, 2018